

Study of EUVL mask defect repair using FIB-GAE method

Tsuyoshi Amano*, Yasushi Nishiyama*, Hiroyuki Shigemura*, Tsuneo Terasawa*, Osamu Suga*,
Kensuke Shiina**, Fumio Aramaki**, Ryoji Hagiwara**, Anto Yasaka**

* MIRAI-Semiconductor Leading Edge Technologies, Inc. (Japan)

** SII NanoTechnology, Inc. (Japan)

16-1 Onogawa, Tsukuba-shi, Ibaraki-ken, 305-8569

Phone: +81-29-849-1479 Fax: +81-29-849-1218 e-mail: amano.tsuyoshi@selete.co.jp

ABSTRACT

We evaluated a new FIB-GAE (Focused Ion Beam-Gas Assisted Etching) repairing process for the absorber defects on EUVL mask. XeF_2 gas and H_2O gas were used as etching assist agent and etching stop agent respectively. The H_2O gas was used to oxidize Ta-nitride side-wall and to inactivate the remaining XeF_2 gas after the completion of defect repair. At the Photomask Japan 2008 we had reported that side-etching of Ta-nitride caused CD degradation in EUVL. In the present paper we report on the performance of defect repair by FIB, and of printability using SFET (Small Field Exposure Tool). The samples evaluated, were in form of bridge defects in hp225nm L/S pattern. The cross sectional SEM images certified that the newly developed H_2O gas process prevented side-etching damage to TaBN layer and made the side-wall close to vertical. The printability also showed excellent results. There were no significant CD changes in the defocus characterization of the defect repaired region. In its defect repair process, the FIB method showed no signs of scan damage on Cr buffered EUV mask. The repair accuracy and the application to narrow pitched pattern are also discussed.

Keywords: EUV, mask, repair, FIB, gas assisted etching, XeF_2 , SFET

1. INTRODUCTION

Extreme ultraviolet lithography (EUVL) is the most promising technology for ULSI devices fabrication that is expected to replace 193-i technology in coming years. However, EUVL still has many challenges to be met e.g., light source power, particle-free mask shipping and handling technologies, development of resist material, defect-free blanks and masks [1], [2], [3], [4], and so on. The feature size requirements for EUVL generation masks are considerably smaller than those for optical lithography. As the feature sizes become smaller, the specifications for pattern defect inspection [5], [6], [7] and defect repair [8], [9] also become more demanding [10], [11], [12].

In the previous EUVL mask repair work with FIB-GAE technology it was reported [9] that opaque defects could be successfully repaired under certain conditions. But the report also said that there remain some technological problems with the FIB technique. One such problem is the implantation of Ga ion into the buffer layer of EUVL mask. The implantation retards the etching rate of the buffer layer and causes residue formation after the completion of the process.

At the Photomask Japan 2008, we reported on the basic repair performance of EUVL mask pattern using the newly developed FIB-GAE repairing techniques focused on the cross-sectional repaired pattern topography after repairing opaque defect. The results proved not only the applicability of FIB-GAE method to EUVL mask but also showed excellent pattern topography after repair, and the etching depth controllability that were regarded as difficult tasks for FIB repairing method.

2. EXPERIMENTAL CONDITION

2.1 Repair tool

We employed a FIB repair tool with gas assisted etching process. Table 1 outlines the basic specifications of the process.

Table 1 The specification of FIB tool

| | |
|------------------------|--------------------------------|
| Repair system: | Prototype system for EUVL mask |
| Acceleration voltage: | 15 kV |
| Probe current: | 2 pA |
| Etching assisting gas: | XeF ₂ gas |
| Etching control gas: | H ₂ O gas |

2.2 EUVL mask structure

A EUV mask used in our repair experiments is shown in Fig. 1. The mask consists of substrate, Mo/Si multilayer, capping layer, buffer layer, and absorber layer including a low reflective layer.

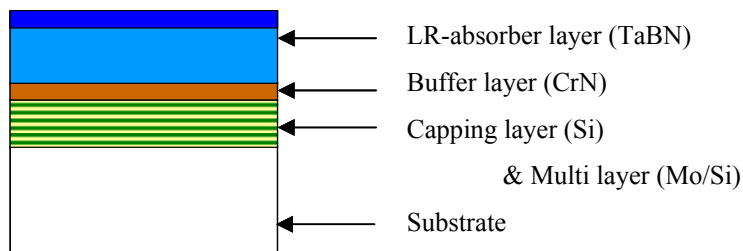
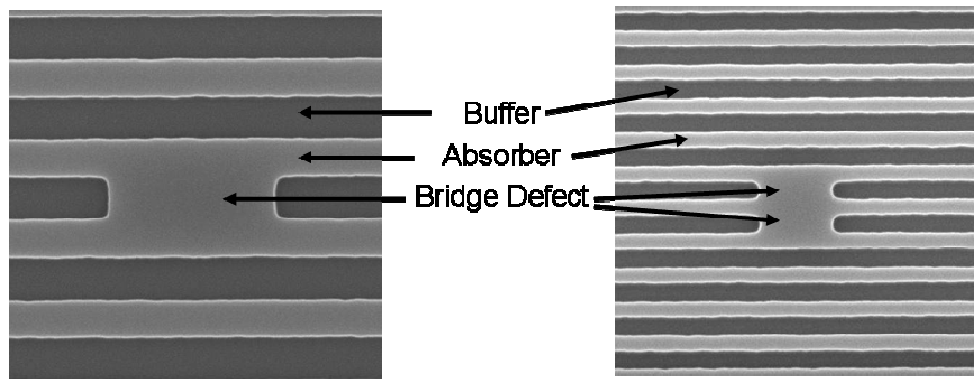


Fig. 1 Structure of sample EUVL mask

2.3 Mask design

Two kinds of test patterns with defects were prepared for the repair experiments. As shown in Figs. 2 (a) and (b), programmed bridge defects were fabricated between adjacent absorber line patterns. The base patterns were hp225nm and hp100nm dense line. The defect types were single bridge and double bridge defects.



a) hp225 nm L/S, defect size 900*225 nm

b) hp100 nm L/S, defect size 400*100 nm

Fig. 2 SEM images of test patterns with bridge defects to be repaired

2.4 Exposure tool and condition

To confirm the usefulness of FIB-GAE method, repaired patterns were printed on a resist coated wafer to study resist pattern width variation. This pattern printing was performed using a small field exposure tool (SFET) shown in Fig. 3. The exposure conditions are shown in Table 2.

Table 2 SFET exposure conditions

| | |
|-----------------|---|
| NA/sigma: | 0.3 (central obscuration 30%), 0.3/ 0.7 (inner/ outer) |
| Magnification: | 1/ 5 |
| Incident angle: | 6 deg. |
| Resist: | SSR3* (*Selete <u>S</u> tandard <u>R</u> esist <u>3</u>) |

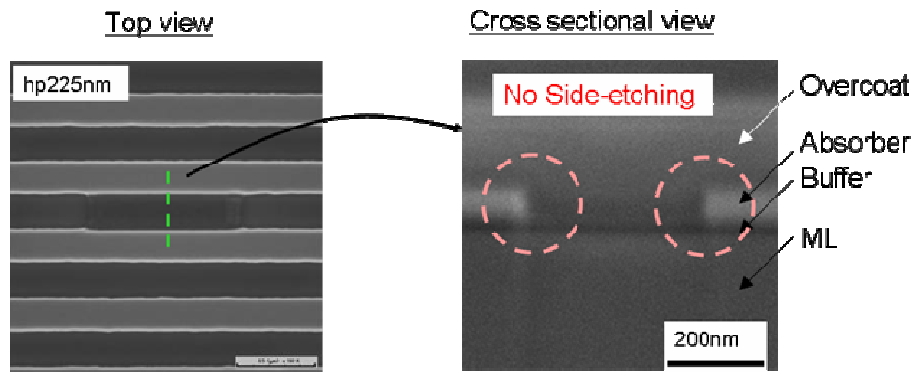


Fig. 3 Photograph of SFET

3. RESULTS AND DISCUSSIONS

3.1 Concept and repair results of new process

The mechanism of side-etching during conventional FIB-GAE or EB repair process is well understood [13] [15] [16]. In the present study, in addition to XeF_2 as etching assist gas, another gas H_2O was also injected, task of which was to terminate the etching process after its completion. The H_2O gas acts not only as an agent to oxidize TaBN side-wall but it also inactivates XeF_2 etching. The sequence of the evaluated repair process was as follows: (1) define defect area, (2) inject XeF_2 gas and irradiate FIB, (3) stop FIB irradiation, and (4) inject H_2O gas immediately. The etching results of repairing by repaired by the improved method are shown in Fig. 3-1. By applying this improved method, bridge defects were completely repaired without any side-etching of the absorber layer, and over etching of the buffer layer. The repair accuracies will be described in sections 3.4 and 3.5.



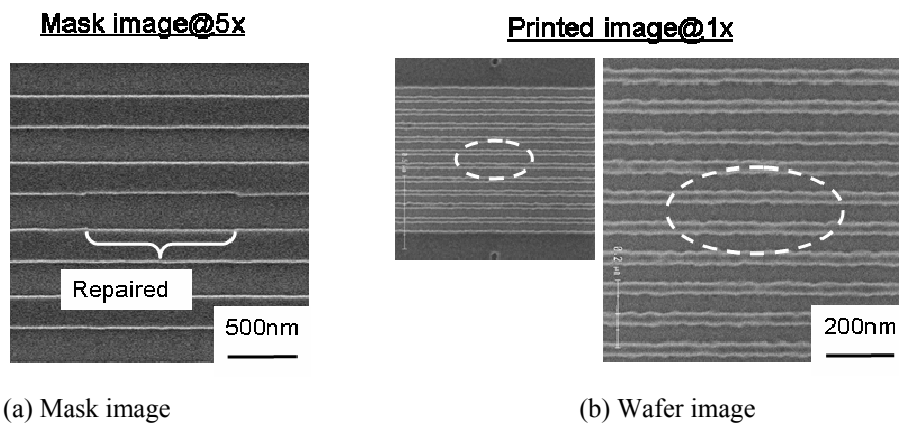
(a) Top view SEM image of repaired area

(b) Cross-sectional SEM image of repaired area

Fig. 3-1 SEM images of bridge defect repaired area after the improved repair process

3.2 Defect printability

Figure 3-2-1 (a) shows an excellent repair result that has no buffer layer residue, and imparts no damage to the capping layer. The defect printability is shown in fig. 3-2-1 (b). While examining for the FIB scan damages, we learned that FIB over-dose causes structural damage to the reflectivity of multilayer resulting in reflectivity loss of EUV light [14]. But the result also indicated that under controlled-dose conditions there was no reflectivity loss around the repaired region. The defocus characteristic of repaired region is shown in fig. 3-2-2. The result also proved that there were no local CD changes around the defect repaired region. These wafer printed results indicate that the FIB-GAE technique has excellent repair performance on Cr buffer type of EUV masks.



(a) Mask image

(b) Wafer image

Fig. 3-2-1 SEM images of the (a) mask and (b) wafer after repairing bridge defect.

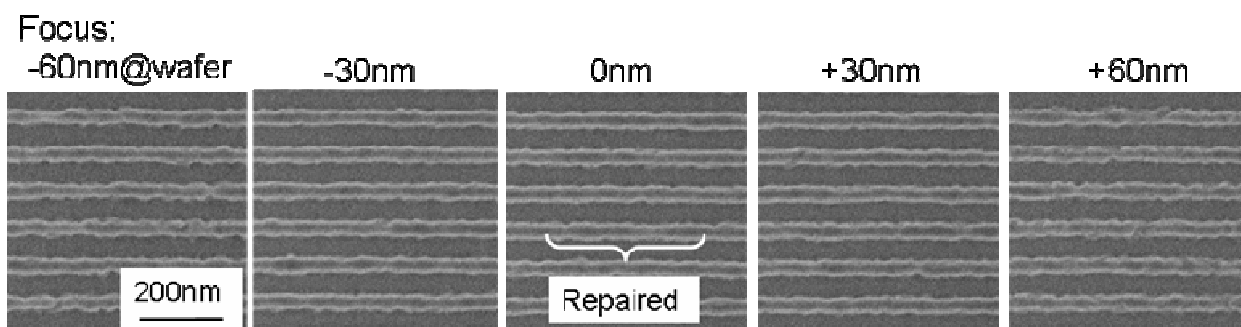
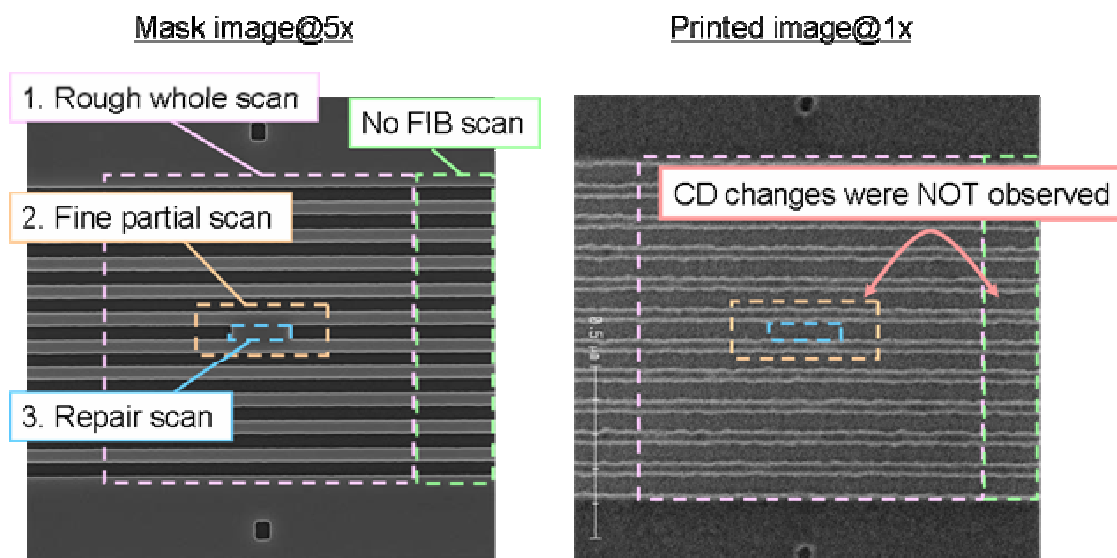


Fig. 3-2-2 Defocus characteristic of the bridge defect repaired region.

3.3 FIB scan damage evaluation

It is of concern that the FIB irradiation causes structural damages to EUV mask. In this section, we evaluated the effect of FIB scanning on image printed on wafer. Normally, during FIB repair process, we have three phases of scan processes. The first phase is rough whole scan to find defects, the second is fine partial scan to define the area to be repaired, and the third is repair scan to etch defects. Fig. 3-3 (a) shows mask image before FIB repair. Each FIB scanning area is indicated in separate boxes. When the FIB dose of rough whole scanned area was defined as unit 1, the relative FIB dose of fine partial scanned was defined as unit 2, and for repair scan the relative dose was 100 or more. Hence there turned out to be three levels of scans that comprised both exposed and un-exposed areas. Fig. 3-3 (b) shows images printed on wafer. In this SEM image, there was seen no significant resist image degradation compared with reference FIB unexposed area which was the case not only with low exposure area but also with high exposure that included the repair scanned area. This result verifies that FIB repair process does not cause any structural damage to Cr buffered EUV mask.



(a) Mask image and FIB scanned area

(b) Wafer image and FIB scanned area

Fig. 3-3 Mask and wafer images for FIB damage evaluation. The mask had bridge defect in hp225nm L/S pattern.

3.4 Placement accuracy

From the stand point of defect repair, the repairing accuracy and controllability are also very important. We repaired five bridge defects in hp225 nm L/S pattern and calculated the repairing placement accuracy. All the repaired samples were captured in 3D profiles using AFM. The edges were defined by the middle height of absorber layer. The placement accuracy was defined as shown in fig. 3-4 (a). The calculated placement accuracy was 10.7 nm in range and 8.7 nm in 3-sigma as shown in Fig. 3-4 (a).

The placement accuracy was good for prototype FIB system. Analysis of variability factor and improvement of repair accuracy will be addressed in future work.

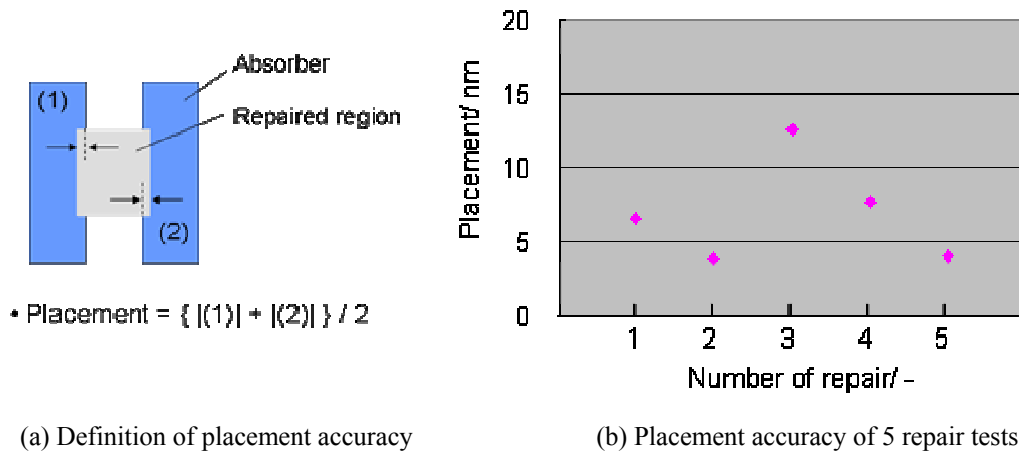


Fig. 3-4 Placement accuracy of bridge defect repair performed with the improved process

3.5 Etching depth controllability

The experimental result on the controllability of etching depth is shown in Fig. 3-5 (b). Here, the depth-zero and negative number mean the surface of buffer layer and the depth away from the surface. The etching depth controllability is one of the most important factors for the success in the development of defect repair. Under the evaluated conditions, the etching selectivity of absorber against the buffer layer was more than 10:1. It exhibited excellent etching depth controllability as shown in Fig. 3-5 (b). The etching end-points were well targeted by the time-controlled etching process. The etching depth controllability was 1.1 nm in range, and 1.3 nm in 3-sigma as shown in Fig. 3-5 (b).

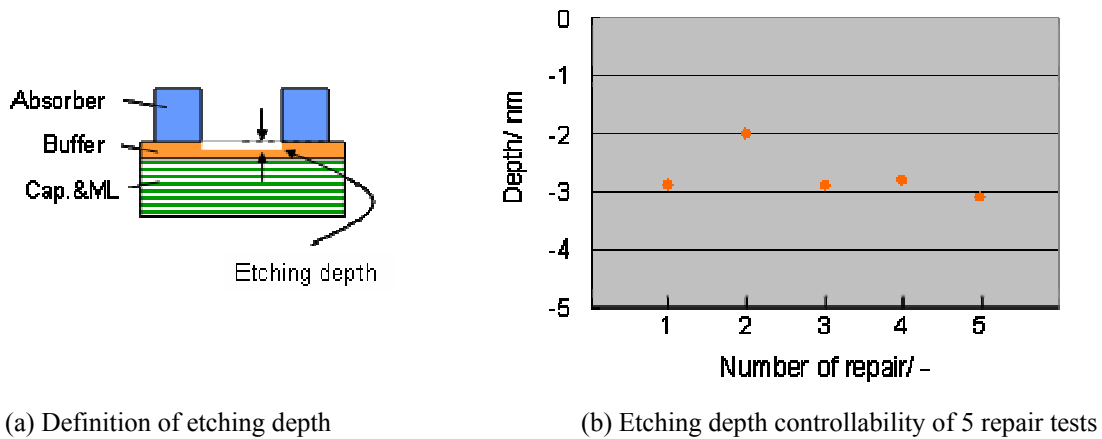
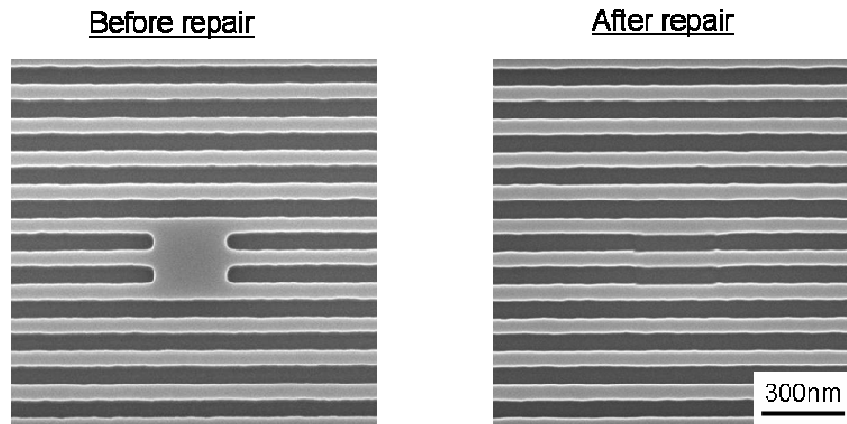


Fig. 3-5 Etching depth controllability of improved process

3.6 Application to hp100 nm dense-line pattern

We have confirmed that absorber defects can be repaired without any side etching damage under the improved FIB-GAE process. To confirm the capability of FIB-GAE on narrow pitched device pattern, we applied the improved repair process to hp100 nm dense-line pattern with 2 bridge-defects like large scale opaque defects. As shown in Fig. 3-6, the defects were successfully repaired. However, small boundary discontinuities between repaired and reference pattern edge also were observed. The SEM image showed that the bridge defects were repaired completely without any side-etching damage. On the boundary discontinuity point, the analysis of the influence of lithography and processing will be addressed in future works.



(a) Top view SEM image of before and after repaired area (b) Tilted view SEM image of repaired area

Fig. 3-6 SEM images of bridge defects before and after the repair process

4. SUMMARY

The newly developed defect repair FIB process can make pattern side-wall to be vertical.

The SFET printed images verified that the bridge defect was completely repaired and no FIB scan damage was observed.

The placement accuracy and etching depth controllability were excellent.

It is confirmed that FIB-GAE technique has good potential for defect repair in hp100 nm L/S pattern.

5. ACKNOWLEDGE

We would like to thank Tsukasa Abe and Tadahiko Takikawa of Dai Nippon Printing Co., Ltd for their mask fabrication support. We would also like to thank Tomokazu Kozakai and Tatsuya Asahata of SII NanoTechnology Inc. for their technical support.

This work was supported by New Energy and Industrial Technology Development Organization (NEDO).

REFERENCES

- [1] T. Hashimoto, et al., "Investigation of Defect Repair Methods for EUVL Mask Blanks through Aerial-Image Simulations" Proc. SPIE vol. 5853, 855, (2005)
- [2] T. Terasawa, et al., "Multilayer bottom topography effect on actinic mask blank inspection signal" Proc. SPIE vol. 6607, 6670K, (2007)
- [3] T. Shoki, et al., "Recent performance of EUV mask blanks with low thermal expansion glass substrates" Proc. SPIE vol. 6730, 673015, (2007)
- [4] K. Hayashi, et al., "Development status of EUVL mask blanks in AGC" Proc. SPIE vol. 6730, 67305D, (2007)
- [5] T. Abe, et al., "EUV mask pattern inspection using current DUV reticle inspection tool" Proc. SPIE vol. 6607, 66070L, (2006)
- [6] D. Y. Kim, et al., "EUV mask pattern inspection for Memory Mask Fabrication in 45nm node and below" Proc. SPIE vol. 6349, 63492L, (2006)
- [7] T. Amano, et al., "Evaluation of EUVL-mask pattern defect inspection using 199-nm inspection optics" Proc. SPIE vol. 6730, 67305J, (2007)
- [8] T. Abe, et al., "Evaluation of dry etching and defect repair of EUVL mask absorber layer" Proc. SPIE vol. 5567, 1435, (2004)
- [9] T. Abe, et al., "Evaluation of defect repair of EUV mask absorber layer" Proc. SPIE vol. 5853, 866, (2005)
- [10] 10. Z. Zhang, et al., "Investigation of resist effects on EUV mask defect printability" Proc. SPIE vol. 6730, 673016, (2007)
- [11] T. Liang, et al., "EUV Mask Pattern Defect Printability" Proc. SPIE vol. 6283, 62830K, (2006)
- [12] H. Aoyama, et al., "Repair specification study for half pitch 32-nm patterns for EUVL" Proc. SPIE vol. 6730, 67305L, (2007)
- [13] B. Li, et al., "Efficient dry etching of Si with vacuum ultraviolet light and XeF₂ in a buffer gas" J. Applied physics 77(1), pp350-356, (1995)
- [14] Y. Nishiyama, et al., "Damage analysis of EUV mask under Ga focused ion beam irradiation" Proc. SPIE vol. 7028, 70280J, (2008)
- [15] T. Amano, et al., "Evaluation of defect repair of EUVL mask pattern using FIB-GAE method" Proc. SPIE vol. 7028, 70281T, (2008)
- [16] Matthew G. Lassiter, et al., "Inhibiting spontaneous etching of nanoscale electron beam induced etching features: Solutions for nanoscale repair of extreme ultraviolet lithography masks" J. Vac. Sci Technol. B 26(3), (2008)